Packaging of up to 240 subunits of a 17 kDa nuclease into the interior of recombinant hepatitis B virus capsids

Gertrud Beterams[a], Bettina Böttcher[b], Michael Nassal[a,*]

[a] *University Hospital Freiburg, Department of Internal Medicine II/Molecular Biology, Hugstetter Str. 55, D-79106 Freiburg, Germany*
[b] *European Molecular Biology Laboratory, Heidelberg, Germany*

Received 15 May 2000; revised 28 June 2000; accepted 1 August 2000

Edited by Hans-Dieter Klenk

Abstract The icosahedral nucleocapsid of hepatitis B virus (HBV) consists of multiple subunits of a single 183 amino acids (aa) core protein encasing the viral genome. However, recombinant core protein alone also forms capsid-like particles. We have recently shown that a 238 aa protein centrally inserted into the core protein can be displayed on the particle surface. Here we demonstrate that replacement of the C-terminal basic domain by the 17 kDa *Staphylococcus aureus* nuclease also yields particles but that in these the foreign domains are located in the interior. The packaged nuclease is enzymatically active, and the chimeric protein forms mosaic particles with the wild-type core protein. Hence the HBV capsid is useful as a molecular platform which, dependent on the fusion site, allows foreign protein domains to either be packaged into or be exposed on the exterior of the particle. These results are of relevance for the use of the HBV capsid as a vaccine carrier, and as a target for antiviral therapy.

Key words: Capsid-like particle; Capsid-targeted viral inactivation; Hepatitis B virus capsid; Particulate vaccine carrier; *Staphylococcus aureus* nuclease

1. Introduction

Hepatitis B virus (HBV), the causative agent of B-type hepatitis in humans [1], is an enveloped DNA-containing virus that replicates through reverse transcription (for reviews: [2–4]). Virion morphogenesis starts with encapsidation by the capsid, or core, protein of a complex consisting of one of the viral RNAs, the reverse transcriptase, and probably cellular chaperones [5]. After reverse transcription, the DNA-containing nucleocapsid buds into a pre-Golgi compartment, exiting from the cell as enveloped virion [6].

Whereas formation of authentic nucleocapsids is thus a complex process, the 183 amino acids (aa) core protein by itself is able to form capsid-like particles upon heterologous expression. Such systems allowed for the biochemical and biophysical characterization of the core protein. The N-terminal 144 aa form the actual assembly domain [7] while the basic C-terminus is required for nucleic acid binding (Fig. 1A). Electron cryo microscopy (cryo EM) revealed two forms of the icosahedrally symmetric capsid [8,9]: the smaller particles (triangulation number $T=3$) contain 180, the larger ones ($T=4$) 240 subunits. The actual building blocks are core protein dimers which adopt a hammer-like structure (Fig. 1A, right). The heads form the capsid shell while the shafts protrude from the surface as spikes. From higher resolution studies [10,11], a model for the fold of the assembly domain was proposed (Fig. 1B, left) which predicted four helices [10]. The two long central helices would be involved in dimerization by forming a four-helix bundle with their counterparts in a second subunit. This model was corroborated biochemically [12,13], and finally confirmed in further detail by the recently solved 3.5 Å X-ray structure [14]. The structure of the basic C-terminus is not known but, as expected from its nucleic acid binding function, it is located in the particle interior [10,15].

Because of its fundamental role in the viral life-cycle, the HBV capsid is a potential target for antiviral therapy (for review: [16]); it is also of interest as a particulate carrier for foreign epitopes that may be suitable as vaccines (for reviews: [17,18]). Various heterologous sequences have been inserted into the core protein with the aim of maintaining the particulate structure while at the same time exposing the foreign sequence on the surface. Additions to the termini of the core protein, in particular to the C-terminus, did frequently not interfere with particle assembly but the immunogenicity of the foreign part was rather low, suggesting it was not well accessible. By contrast, insertions into the central immunodominant c/e1 epitope region around aa 80 (Fig. 1B) at the tips of the surface spikes [19] were often highly immunogenic but the assembly-competence of such variants appeared to be restricted to relatively short to medium-sized [20] inserts. However, we have recently demonstrated that insertion of the entire green fluorescent protein (GFP) into this site yields particles that display GFP on their surface [21]. Here we asked whether, by appropriate design, the HBV capsid could also be used to package multiple copies of a substantially sized protein into its interior. As a model, we used the nuclease (Fig. 1C) of *Staphylococcus aureus* (SN), a globular 17 kDa protein [22] that degrades DNA and RNA in a Ca^{2+}-dependent fashion [23]. Below we show that a chimeric protein containing the entire SN protein fused to the C-terminus of the core protein's assembly domain indeed meets these criteria.

2. Materials and methods

2.1. Plasmid constructs

The parental construct for HBV core protein expression, plasmid pPLC4-1 [24], contains a synthetic core gene under control of the phage lambda pL promoter. Using plasmid pTSN2cc (kindly provided by J. Markley) as template and appropriate oligonucleotide primers, a PCR product encoding the nuclease A part of SN (V8 strain containing the H124L mutation), preceded by 6 aa from the authentic pro-

*Corresponding author. Fax: (49)-761-270 3507.
E-mail: nassal2@ukl.uni-freiburg.de

0014-5793/00/$20.00
PII: S0014-5793(00)01927-X

peptide and followed by a C-terminal His6 tag, was obtained. This fragment was cloned by standard procedures between the *Bst*EII (position 461) and *Hin*dIII (position 555) of pPLC4-1, yielding plasmid pPLC-SNwt. The encoded protein, coreSNwt, consists of HBV core protein aa 1–155, a two aa linker, and tagged SN as described above. Fusions with enzymatically disabled SN domains [25,26], coreSNmut87 and coreSNmut43/87, were obtained by introduction into SN of aa exchanges R87G alone (plasmid pPLC-SNmut87), or in combination with E43S (plasmid pPLC-SNmut43/87). For co-expression, plasmid pDM/c1–183 (M. Nassal and A. Frank, unpublished data) was used which encodes wild-type HBV core protein c1–183 under control of the bacteriophage T7 A1 promoter coupled to two lac operators; this A1/O4/O3 promoter, as present in the pUHE plasmids derived from the pDS series [27], is inducible by IPTG. The plasmid carries the lacI^q allele of the lac repressor, the P15A replication origin from pACYC184, and confers resistance to kanamycin. Hence both plasmids can be maintained in the same cell, and protein expression can be separately induced.

2.2. Expression of variant and wild-type HBV core proteins

Expression experiments were performed in *Escherichia coli* GI698 cells (Invitrogen) by tryptophan induction (100 μg/ml) as previously described [12]. In co-expression experiments, transcription from plasmid pDM/c1–183 was induced by addition of IPTG (final concentration 1 mM). Usually, bacterial cultures were grown at 30°C to mid-log phase (about 0.5 OD 550 nm), then inductor was added and the cultures were maintained at 23°C for about 16 h.

2.3. Purification of recombinant proteins

Induced bacterial cultures were lysed by lysozyme/detergent treatment and sonication as previously described [12]. Core protein derivatives were precipitated using 40% saturated ammonium sulphate, redissolved in phosphate-buffered saline (PBS) buffer (10 mM Na_2HPO_4, 2 mM NaH_2PO_4, 140 mM NaCl), and after dialysis subjected to sedimentation in sucrose gradients consisting of six layers of 10–60% (w/v) sucrose in PBS. For preparative gradients, each sucrose layer consisted of 2 ml, and 800 μl of cleared dialysate was loaded and centrifuged at 20°C for 105 min at 41 kRPM in a TST 41.14 rotor (Kontron). For analytical gradients, each sucrose layer as well as the sample had a volume of 200 μl. Centrifugation conditions were 20°C, 40 min, 55 kRPM in a TLS55 rotor (Beckman). Gradients were fractionated from top to bottom. Protein contents of individual fractions were analyzed by sodium dodecyl sulphate (SDS)–PAGE (12.5% polyacrylamide, 0.1% SDS; [28]) followed by Coomassie blue staining or Western blotting onto Hybond-P PVDF membranes and chemiluminescence detection (ECL Plus; both Amersham Pharmacia) using appropriate primary and secondary antibodies.

2.4. Native agarose gel electrophoresis of recombinant particles

Aliquots from individual gradient fractions were subjected to electrophoresis in native agarose gels (0.5–1%) as previously described [7,12,21]. As running buffer, TAE (40 mM Tris–acetate pH 8.1, 0.1 mM EDTA) containing 0.5 μg/ml ethidium bromide was used. Nucleic acids were visualized by illumination at 365 nm. Proteins were detected directly by Coomassie blue staining, or by immunoblotting after capillary transfer to PVDF membranes as described above.

2.5. Dissociation of chimeric particles

Equal aliquots from gradient-purified particle preparations were dialyzed against either 3 M urea in 25 mM Tris–Cl$^-$ pH 9.5, or against TN buffer (10 mM Tris–Cl$^-$, pH 7.5, 100 mM NaCl) and resedimented in sucrose gradients made up with the same buffers. For the nuclease assays described below, proteins from the top fractions (urea-treated) and from the particle-specific lower fractions (TN-incubated) were used.

2.6. Nuclease activity assays

Nuclease activity was determined by using covalently closed circular (ccc) plasmid DNA as substrate [25], and monitoring the disappearance of cccDNA and the concomitant generation of open circular (oc) and linear DNAs by agarose gel electrophoresis (1% agarose, TAE buffer). Reaction mixtures contained, in a total volume of 200 μl TN buffer, 20 μg of a 5.3 kb plasmid DNA (5.7 pmol), 10 mM $CaCl_2$ and approximately 2.5 ng (0.07 pmol) of coreSN protein (obtained by resedimentation after TN or urea incubation as described above).

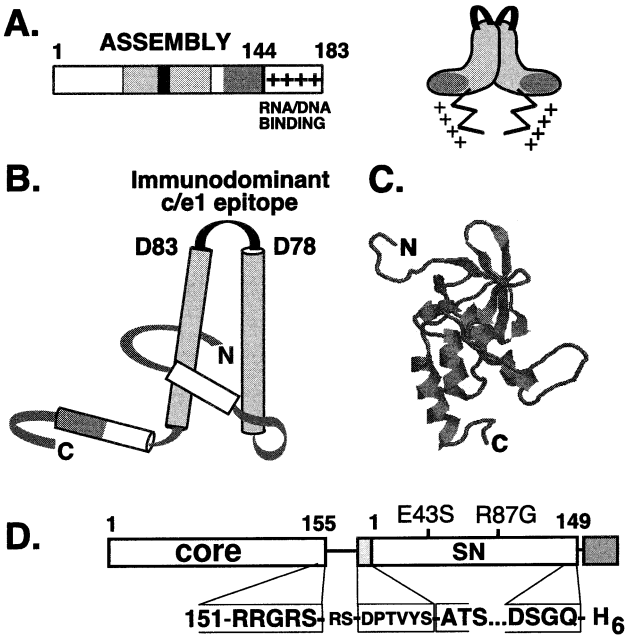

Fig. 1. Structures of the HBV core protein and of *S. aureus* nuclease. A: Primary sequence of the core protein and schematic representation of the core protein dimer. The assembly domain extends from the N-terminus to about aa 144, followed by a basic nucleic acid binding domain (marked by ++). The black box depicts the immuno-dominant c/e1 epitope region. Gray shading refers to the approximate location of the corresponding sequences in the topological dimer model (right). Two assembly domains associate into a hammer-shaped dimer. The c/e1 epitope (black loop) is located at the tip of the spike. The basic C-termini (++) are directed into the particle interior. B: Structural model of the core protein. The cylinders represent the major core protein helices; gray shading is as in A. C: Structure of SN. The RasMol representation is based on a 1.5 Å X-ray structure of SN [22], and comprises residues 1–141 of mature nuclease A. Scales in B and C are similar. D: Linear representation of the coreSN fusion proteins used in this study. The core protein part encompasses the sequence 1–155 to which mature SN 1–149, preceded by 6 aa from the authentic propeptide and followed by a His6 tag, is joined via a 2 aa linker. Two variants with essentially inactive SN domains contain the mutations R87G, and E43S+R87G.

Mixtures were incubated at 37°C. 15 μl aliquots were removed after 0.5, 1, 2, 3, 4, 5, 10, 20 and 30 min and EDTA was immediately added to 50 mM to stop the reaction. As control, 1.2 ng per assay (0.07 pmol) of a commercial SN preparation (Amersham Pharmacia USB; specific activity: 17 U/μg) was used. To account for possible effects of urea on nuclease and/or substrate, control assays were performed using SN that had been incubated for 1 h with 3 M urea in 25 mM Tris–Cl$^-$ pH 9.5. For quantitation, pictures of the ethidium bromide-stained gels were taken using a DIANA CCD camera, and cccDNA band intensities were determined using AIDA software (both Raytest). Curves were fit exponentially using Microsoft Excel. Nuclease activity against packaged RNA was induced by addition to gradient-purified particles of $CaCl_2$ to a final concentration of 10 mM.

2.7. Antibodies

For detection of HBV core protein, the following antibodies were used: H800, a polyclonal rabbit antiserum raised against denatured c1–149 protein [7]; monoclonal antibodies mc312 [29] and mc275 [30], recognizing the major c/e1 epitope, and a particle-specific conformational epitope, respectively. His tags were detected using the tetra-His monoclonal antibody (Qiagen).

2.8. EM

For negative staining, 2 μl of a solution containing the gradient-purified particles was applied to a carbon-coated copper grid and

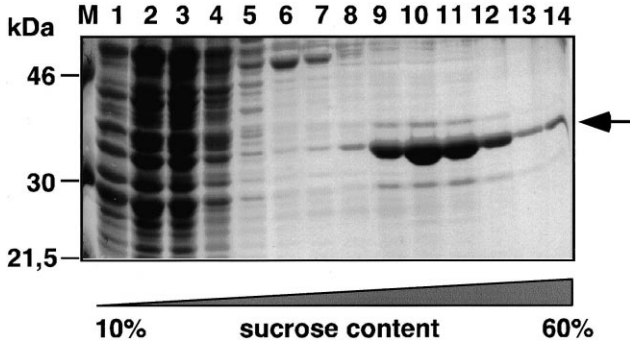

Fig. 2. The chimeric coreSNwt protein is assembly-competent. Cleared lysate from an induced culture of *E. coli* cells transformed with plasmid pPLC-SNwt was centrifuged through a 10–60% sucrose gradient in PBS buffer. Aliquots from individual gradient fractions were analyzed by SDS–PAGE and stained with Coomassie blue. The bulk of the 36 kDa coreSNwt protein is present in fractions 9–12 characteristic for particles.

incubated for approximately 1 min. The grid was washed twice with water and twice with 2% uranyl acetate and finally stained for 1 min with 2% uranyl acetate. Micrographs were taken on a Philips EM 400 operating at 100 kV at a nominal magnification of 55 000. For cryo EM, aliquots from appropriate sucrose gradient fractions were dialyzed against PBS buffer, then concentrated to about 2–5 mg/ml protein using a Centricon 500 microconcentrator (Millipore). Sample preparation and microscopy were carried out as described [10] using a Hitachi HF2000 equipped with a Gatan cold stage. The temperature of the stage was maintained between 97 and 100 K. Micrographs were taken under low dose conditions at a nominal magnification of 60 000 with a 2 s exposure time.

3. Results

3.1. Chimeric coreSN proteins form particles

The structures of the coreSNwt protein and its enzymatically disabled variants serving as controls for nuclease-specific effects are shown in Fig. 1C. All proteins were expressed in substantial amounts in *E. coli* GI698 cells (about 10 mg/l of bacterial culture), and their identity was confirmed by Western blotting with monoclonal antibodies against core protein and the C-terminal His tag (not shown). As a first test whether the chimeric coreSN proteins are able to form particles, cleared bacterial lysates were sedimented through sucrose gradients. As shown in Fig. 2 for the coreSNwt fusion, most of the 36 kDa chimeric protein was present in fractions that are characteristic for the particulate form; both coreSN-mut proteins displayed essentially the same sedimentation behavior.

An independent method to detect particle formation is native agarose gel electrophoresis [31]. Stable wild-type HBV capsids migrate as distinct bands through the gel matrix [7]. However, all coreSN proteins appeared as a relatively broad smear, with only the leading edge migrating close to the position of wild-type core particles. While compatible with the presence of particles with decreased stability [12], the experiments did not conclusively confirm particle formation. However, the distinct mobility was useful for the detection of mosaic particles formed upon co-expression with wild-type core protein (see below and Fig. 5B).

In order to obtain definite proof for the assembly-competence of the fusion proteins, we used EM, and compared the

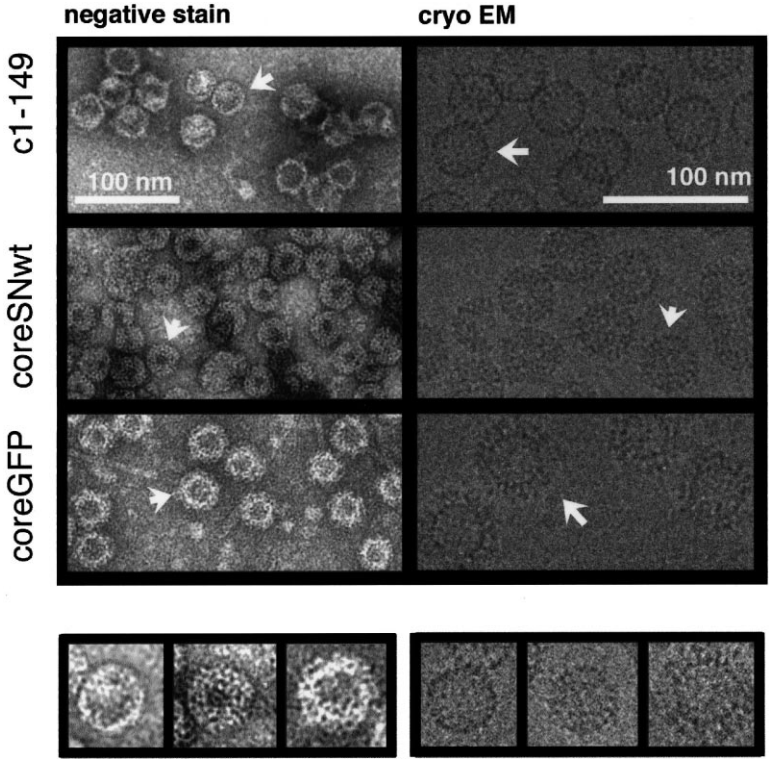

Fig. 3. EM of coreSNwt particles. Particles from truncated wild-type core protein c1–149, and from the chimeric proteins coreSNwt and coreGFP were analyzed by negative staining with uranyl acetate (left panels), or by cryo EM (right panels). Magnification is the same within one series but differs between the left and right panels. The naturally low contrast of the cryo electron micrographs is due to the low atomic masses of the constituent elements of proteins. A blow-up of single particles, indicated by the white arrows, is shown at the bottom; left to right order corresponds to top to bottom in the large pictures.

material from the particle-specific coreSNwt gradient fractions with particles formed by the truncated wild-type core protein c1–149, and with coreGFP particles that expose the GFP domains on their surface [21]. Negative staining with uranyl acetate (Fig. 3, left panels) revealed abundant particles in the coreSNwt preparations, with two distinct features: (i) their overall size was similar to that of authentic c1–149 capsids but smaller than that of chimeric coreGFP particles; in turn, the apparent thickness of the capsid shells was increased; (ii) a substantial fraction of the particles were deformed to some degree. The micrographs obtained with the chimeras containing mutant SN domains were basically identical (not shown). Different from negative staining, in cryo EM, the specimens are observed under quasi-native conditions (for review: [32]). The diameter of the chimeric particles (Fig. 3, right panels) was again similar to that of wild-type capsids, but they appeared much more regularly shaped than after negative staining; as for the c1–149 capsids, there were much more $T=4$ than $T=3$ particles. A direct comparison of single, typical particles observed by either technique is shown at the bottom of Fig. 3. Hence these data provide direct evidence for the assembly-competence of the coreSN protein, and they strongly suggest that the SN domains are packaged in the lumen of the particles. This was corroborated by radial density plots (not shown): both coreSN and c1–149 displayed the strongest peaks at a radius of about 143 Å, corresponding to the region of highest capsid shell density, but only coreSN produced additional density peaks at radii of around 77 Å and 108 Å, i.e. inside the shell; coreGFP particles, by contrast, produced an additional outer density peak at about 186 Å.

3.2. The SN domain in the chimeric protein is enzymatically active

To show that the SN domains were correctly folded, and to obtain independent evidence for their interior location, we tested the nuclease activity of the coreSNwt protein with and without subjecting the particles to 3 M urea in 25 mM Tris–Cl^- pH 9.5, a treatment expected to lead to dissociation into dimers [33]. This should increase rather than decrease nuclease activity because the SN domains buried in the particle would gain access to the substrate. Purified coreSN and coreSNmut particles were dialyzed against the above described buffer and, for control, against TN buffer. After resedimentation through sucrose gradients, aliquots from a top fraction from the dissociated material, and from a particle fraction of the control preparation containing equal amounts of fusion protein were used. A commercial preparation of SN at approximately the same molar concentration served as a positive control. To account for the potential influence of urea on nuclease activity, the SN used for comparison with the dissociated coreSN particles was also pretreated with 3 M urea.

Nuclease activity was assayed using the distinct electrophoretic mobilities of oc and linear forms of plasmid DNA generated by nucleolytic attack on cccDNA [25]. Visual inspection of the gels revealed that the cccDNA was much more slowly converted into oc and linear DNA by the native coreSN particles than by native SN (Fig. 4A, left panels). By contrast, the urea-treated chimera showed a largely increased activity, exceeding that of urea-treated SN (right panels). Expectedly, the coreSNmut chimeras displayed no activity (not shown). For a semi-quantitative evaluation, the bands corresponding to cccDNA were densitometrically scanned, and their intensities were plotted vs. reaction time (Fig. 4B). Relative reaction velocities were determined from the slopes between initial time points. Urea treatment of the coreSNwt particles increased the initial velocity by about 8.5-fold whereas that of SN itself dropped about 2.5-fold (from 15-fold to 6-fold faster than with the native coreSNwt particles). Considering this negative influence of urea on SN enzyme activity, this indicates an about 20-fold increase in the apparent activity of the chimeric coreSNwt protein after particle dissociation, consistent with the internal localization of the SN domains. Comparable results were obtained when denatured herring sperm DNA was used as substrate and the release of acid-soluble material was measured photometrically (data not shown).

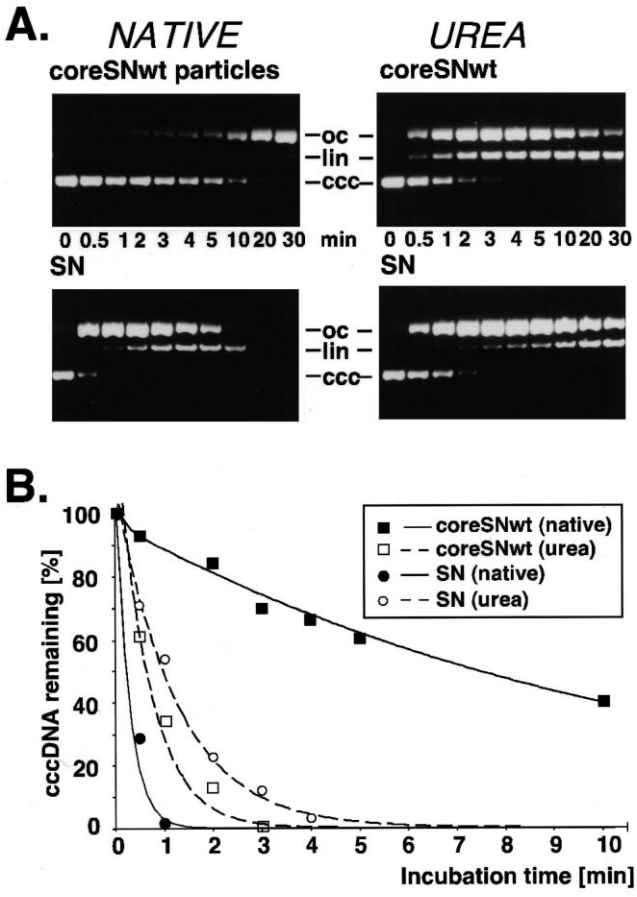

Fig. 4. Increased nuclease activity of coreSNwt after particle dissociation. A: Plasmid cccDNA conversion assay. Gradient-purified coreSNwt particles were treated with either 3 M urea or with buffer, and resedimented on sucrose gradients. Equal amounts of dissociated (marked UREA) and of particulate (buffer control, marked NATIVE) protein were incubated with plasmid cccDNA. Urea-treated and non-treated SN at the same concentration served as control. Samples were taken at the indicated times and the disappearance of cccDNA (marked ccc) and concomitant generation of oc and linear DNA (marked oc and lin) were monitored by agarose gel electrophoresis and ethidium bromide staining. B: Semi-quantitative evaluation of relative reaction rates. The intensities of the cccDNA bands in each lane were determined densitometrically. The values, with the intensity at 0 time in each series set to 100%, were plotted vs. incubation time. Exponential fitting was used to derive the curves shown.

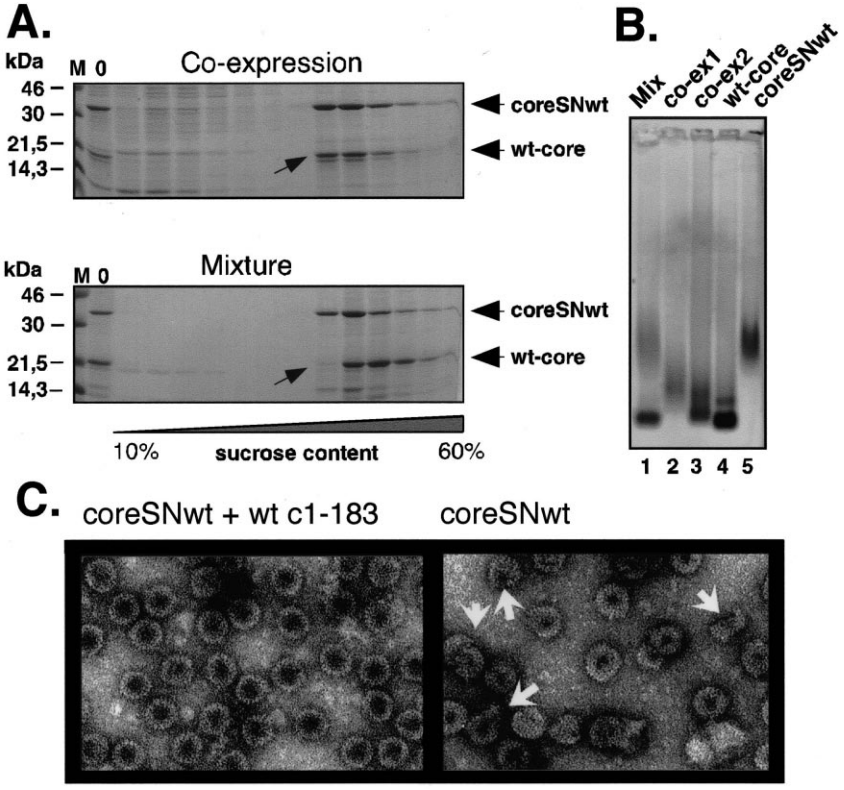

Fig. 5. Evidence for mosaic particle formation from coreSNwt and wild-type c1–183 proteins. A: Sedimentation velocity. Co-expressed coreSNwt plus wild-type c1–183 protein (upper panel) or a mixture of the separately expressed proteins were sedimented through a sucrose gradient. M denotes marker proteins of the indicated sizes, lane 0 is an aliquot of the samples loaded on the gradient. Fractions were analyzed by SDS–PAGE and stained with Coomassie blue. The co-expressed proteins co-sedimented, whereas the peaks of the two proteins were shifted in the mixture (arrows). B: Native agarose gel electrophoresis. Aliquots from particle-specific gradient fractions were subjected to electrophoresis in 0.5% agarose gels, and the proteins were stained with Coomassie blue. On lanes 4 and 5, separately expressed wild-type c1–183 core (wt-core) and coreSNwt protein were loaded, lane 1 (Mix) contained a mixture of the two. Lanes 2 and 3 are derived from co-expression. The material in lane 2 contained about equimolar amounts of both proteins, in lane 3, wild-type core protein was present in an about 4-fold molar excess. C: EM analysis of mosaic particles. Co-expressed coreSNwt plus wild-type c1–183 particles and individually expressed coreSNwt particles were analyzed in parallel by negative staining. Note the uniform particle appearance upon co-expression compared to the frequently distorted and/or incomplete particles (arrows) in the coreSNwt preparation.

3.3. Chimeric coreSN proteins co-assemble with wild-type core protein to form mosaic particles

To test whether the coreSN proteins were able to co-assemble with the wild-type core protein, both were simultaneously expressed in the same *E. coli* cells. The expression products were purified and analyzed as described above. SDS–PAGE of sucrose gradient fractions showed that in all cases the 21 kDa wild-type core protein and the 36 kDa chimera co-sedimented (Fig. 5A, upper left panel). By contrast, a mixture of prepurified wild-type and chimeric capsids showed a slight but distinct shift in the peak positions of the two proteins (lower left panel). Further evidence for the presence of mosaic particles was obtained by native agarose gel electrophoresis (Fig. 5B). A mixture of pure wild-type core protein and coreSNwt (lane 1) showed the same different mobilities as the individual proteins (lanes 4 and 5). By contrast, when coreSNwt was co-expressed at about equimolar concentration with wild-type core protein, one broad band was observed that moved closer to the position of wild-type particles (lane 2), and the material condensed into a distinct, wild-type-like band when the wild-type core protein was present in about 3–4-fold excess over coreSNwt (lane 3). This gradual mobility shift indicated that mixed particles had formed. This conclusion was corroborated by negative staining EM which revealed again abundant particles with a very similar appearance in all preparations (Fig. 5C). They looked much more uniform and regular than those formed from pure coreSN protein.

3.4. The SN domains inside mosaic particles are enzymatically active

Particles from full-length wild-type core protein package substantial amounts of *E. coli* RNA which can be detected in situ by native agarose gel electrophoresis in the presence of ethidium bromide. Particles from the truncated variants lacking the basic C-terminal region, by contrast, contain relatively little nucleic acid [7]. Chimeric coreSN particles per se are therefore not expected to carry packaged nucleic acid while in mixed particles the wild-type protein may bring in detectable amounts of RNA. Accordingly, particle preparations from wild-type core protein, from the chimeric coreSNwt and coreSNmut87 proteins, and from co-expressions were analyzed side-by-side using the native gel assay (Fig. 6, upper panel). For an estimate of the protein amounts present in each lane, the gels were subsequently stained with Coomassie blue (Fig. 6, lower panel). Since similar amounts of protein were present in all samples, the intensity of the ethidium bromide stain is an approximate measure for the relative amounts of nucleic acid per particle. Expectedly, pure wild-type core par-

ticles gave a strong signal (lane 1a) whereas no or only a minimal staining was observed with pure coreSNwt and coreSNmut (lanes 2a and 3a). The mosaic particles, by contrast, were clearly stained; this staining was more intense for particles containing the enzymatically inactive coreSNmut (compare lanes 4a and 5a). Pretreatment with exogenously added RNase A did not abolish staining (lanes 1b–5b), suggesting that most of the visible RNA was protected, i.e. encapsidated. As previously observed [7], protection was not absolute but, importantly, the difference between the mixed particles containing coreSNwt, or coreSNmut87, was maintained. This suggests the active nuclease of the coreSNwt protein had already digested part of the RNA, either in the bacteria or during work-up.

Because SN activity is Ca^{2+}-dependent, we also incubated the particle preparations with 10 mM $CaCl_2$ before loading the samples. This pretreatment had no effect on the staining intensity of wild-type core particles and on the mosaic particles containing the inactive coreSNmut protein (Fig. 6, lanes 1c and 5c). By contrast, the residual staining of the coreSNwt-containing material was completely abolished (lane 4c), indicating Ca^{2+}-dependent activation of the SN domains. In addition, the treatment induced a drastic mobility shift specifically for the coreSNwt chimera (compare lanes 4a and 4b to 4c in the Coomassie stain). This result is consistent with the Ca^{2+}-induced elimination of the particle-stabilizing interactions between the packaged RNA and the basic C-termini of the wt-core protein subunits. Together, these data indicate that the SN domains inside the particle are active and properly folded, and that they can be activated by exogenous addition of Ca^{2+}-ions.

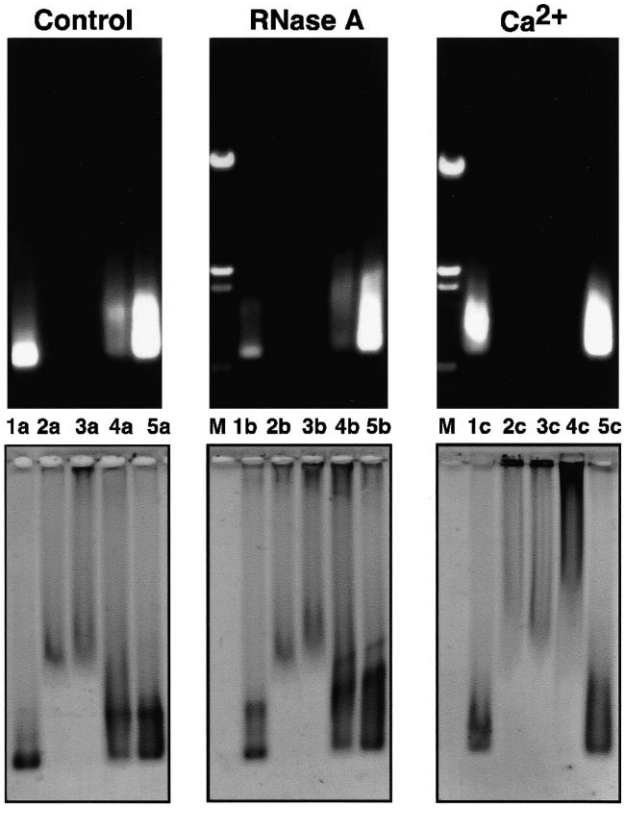

Fig. 6. Ca^{2+}-dependent activity of the SN domains in coreSNwt/c1–183 mosaic particles. Particle preparations from pure proteins wild-type c1–183 (lanes 1), coreSNwt (lanes 2), coreSNmut87 (lanes 3), and from coreSNwt and coreSNmut87 co-expressed with wild-type c1–183 at a 1:4 ratio (lanes 4 and 5) were incubated with PBS buffer (control), or RNase A, or 10 mM $CaCl_2$ as indicated, then analyzed in parallel by native agarose gel electrophoresis. Nucleic acids were visualized by ethidium bromide staining (upper panel), proteins by Coomassie blue staining (lower panel). M denotes a DNA size marker. All samples containing wild-type core protein (lanes 1, 4 and 5) but not those consisting of only chimeric proteins (lanes 2 and 3) showed a strong ethidium bromide staining that co-localized with the bulk of protein. The staining was largely resistant to RNase A while $CaCl_2$ led to a complete loss of staining of the mosaic particles carrying SNwt domains, accompanied by a drastic mobility shift (lane 4a vs. 4c); mosaic particles with SNmut domains remained unaffected (lane 5a vs. 5c).

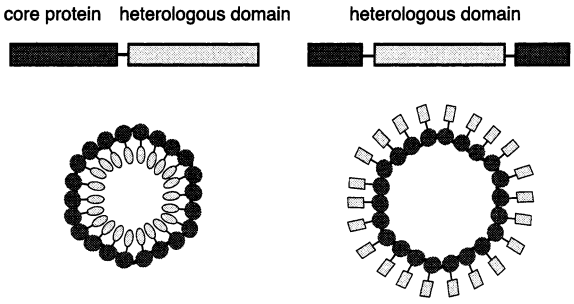

Fig. 7. The HBV capsid as an icosahedral scaffold for foreign protein domains. Depending on the junction site, the HBV core protein can be used to generate particles that either package the heterologous domains into their interior (left: fusion to the C-terminal end of the assembly domain) as shown here for SN, or that display the foreign domains on their surface (right: insertion into the central c/e1 epitope region), as previously demonstrated for GFP.

4. Discussion

In this report, we show that (i) foreign protein domains of similar size and number to the core protein subunits in the HBV capsid can be packaged into the particle interior by fusion to the C-terminal end of the core protein's assembly domain; (ii) the foreign domains are, at least in part, properly folded as shown by enzymatic activity in the dissociated state as well as inside the particle; (iii) the chimeric protein can co-assemble with the wild-type core protein; (iv) the SN domains inside the particle can be activated by exogenously added Ca^{2+}, leading to degradation of the packaged *E. coli* RNA.

The assembly-competence of the coreSN fusion proteins per se was demonstrated by their fast sedimentation, and by direct visualization of abundant particles by negative staining and by cryo EM. The native agarose gel assay, in this case, could not be used to prove particle formation. Possibly, the steric stress induced by the large foreign domains destabilizes the particles such that they disintegrate under the conditions of gel electrophoresis, as previously observed with some core protein point variants [12]. This view is also supported by the frequently deformed appearance of neat coreSN particles in negative staining where the sample is treated with heavy metal salts at low pH, while the particles appeared more regular under the near-native conditions of cryo EM.

The internal localization of the SN domains is supported by several lines of evidence. In the EM analysis, the diameter of the chimeric particles was about equal to that of wild-type cores; by contrast, coreGFP particles with their surface exposed GFP domains are larger (Fig. 3). In addition, the chimeric capsid shells appeared much thicker than those of the

wild-type protein. This has been further confirmed in the meantime by a low resolution three-dimensional reconstruction that revealed extra mass inside but not on the surface of the chimeric particles. Independently, the about 20-fold increased nuclease activity upon treatment with partially denaturing conditions fully supports an interior location of the SN domains.

How plausible is it that the lumen of the HBV capsid can accommodate about 4 MDa of foreign protein mass? The radius of the inner capsid lumen is around 13 nm [14]. For a regular sphere, this amounts to a volume of roughly 9000 nm^3. The dimensions of native SN are about $4\times3\times3$ nm (D. Shortle, personal communication), hence the volume of one subunit corresponds to about 36 nm^3, and that of 240 subunits to about 8600 nm^3. Not considering packing problems, this estimate suggests that there is indeed sufficient space for all SN domains (but probably not for a similar number of much larger protein domains).

The ability of the chimeric coreSN protein to co-assemble with wild-type core protein was demonstrated by co-sedimentation, by native agarose gel electrophoresis and by the uniform appearance of the particles by conventional EM. Moreover, the sensitivity of the RNA contained in these particles toward activation of the SN domains by Ca^{2+}-ions (Fig. 6) demonstrates that the coreSN domains are directed into their interior.

The results described above have several implications. Together with our recent demonstration that the entire GFP can be natively displayed on the surface of the HBV capsid [21], the current study shows that the capsid can be used as a macromolecular platform to force up to 240 foreign protein domains into an ordered superstructure, at will either inside, or on the surface of the icosahedral capsid frame (Fig. 7).

In addition, our data may be relevant to the application of the HBV capsid as a tool in vaccine development, and as a target for antiviral therapy. Authentic HBV capsids can act as T cell-independent antigens because the repetitive display of identical structural features on the particle surface directly activates B cells [34]. To exploit this fact for vaccines, heterologous sequences should be inserted into the immuno-dominant c/e1 epitope region rather than at the C-terminal end of the assembly domain. Our data are consistent with the view that the low immunogenicity of a number of foreign peptides attached to the latter site [18] is due to their interior localization in the capsid, at least up to a certain size. Whether larger foreign domains might be directed to the particle surface remains to be determined. We do not exclude this possibility because the region around aa 150 is part of a flexible hinge connecting the assembly and the nucleic acid binding domains [35]; unfortunately, this region was not visible, or absent, respectively, in the capsids used for X-ray analysis [14].

The HBV capsid is also a potential target for therapy [16]. A conceptually powerful strategy is that of 'capsid-targeted viral inactivation' [36] which, by fusion to a viral structural protein, aims at directing a degradative enzyme specifically into virus particles. Its principal feasibility has been demonstrated using the yeast retrotransposon Ty1 [37], and the Moloney murine leukemia virus model system [38,39]. The properties of the coreSN chimera described in this study suggest it as an attractive candidate for the application of this strategy to HBV, and experiments to confirm its antiviral activity are underway.

Acknowledgements: We thank John Markley, University of Wisconsin, Madison, for providing the cloned SN gene used in this study. This work was supported in part by Grants from the Deutsche Forschungsgemeinschaft (DFG Na154/5-1), the Bundesministerium für Bildung und Forschung (BMBF 01KV9804/1), and the Fonds der Chemischen Industrie.

References

[1] Blumberg, B.S. (1997) Proc. Natl. Acad. Sci. USA 94, 7121–7125.
[2] Nassal, M. and Schaller, H. (1996) J. Viral Hepat. 3, 217–226.
[3] Nassal, M. (1999) Intervirology 42, 100–116.
[4] Nassal, M. (2000) in: Frontiers in Molecular Biology, Vol. 26, DNA Virus Replication (Cann, A., Ed.), pp. 1–40, Oxford University Press, Oxford.
[5] Hu, J., Toft, D.O. and Seeger, C. (1997) EMBO J. 16, 59–68.
[6] Bruss, V., Gerhardt, E., Vieluf, K. and Wunderlich, G. (1996) Intervirology 39, 23–31.
[7] Birnbaum, F. and Nassal, M. (1990) J. Virol. 64, 3319–3330.
[8] Crowther, R.A., Kiselev, N.A., Böttcher, B., Berriman, J.A., Borisova, G.P., Ose, V. and Pumpens, P. (1994) Cell 77, 943–950.
[9] Kenney, J.M., von Bonsdorff, C.H., Nassal, M. and Fuller, S.D. (1995) Structure 3, 1009–1019.
[10] Böttcher, B., Wynne, S.A. and Crowther, R.A. (1997) Nature 386, 88–91.
[11] Conway, J.F., Cheng, N., Zlotnick, A., Wingfield, P.T., Stahl, S.J. and Steven, A.C. (1997) Nature 386, 91–94.
[12] König, S., Beterams, G. and Nassal, M. (1998) J. Virol. 72, 4997–5005.
[13] Koschel, M., Thomssen, R. and Bruss, V. (1999) J. Virol. 73, 2153–2160.
[14] Wynne, S.A., Crowther, R.A. and Leslie, A.G. (1999) Mol. Cell 3, 771–780.
[15] Zlotnick, A., Cheng, N., Stahl, S.J., Conway, J.F., Steven, A.C. and Wingfield, P.T. (1997) Proc. Natl. Acad. Sci. USA 94, 9556–9561.
[16] Nassal, M. (1997) Arch. Virol. 142, 611–628.
[17] Milich, D.R., Peterson, D.L., Zheng, J., Hughes, J.L., Wirtz, R. and Schodel, F. (1995) Ann. N.Y. Acad. Sci. 754, 187–201.
[18] Ulrich, R., Nassal, M., Meisel, H. and Krüger, D.H. (1998) Adv. Virus Res. 50, 141–182.
[19] Conway, J.F. et al. (1998) J. Mol. Biol. 279, 1111–1121.
[20] Koletzki, D., Biel, S.S., Meisel, H., Nugel, E., Gelderblom, H.R., Krüger, D.H. and Ulrich, R. (1999) Biol. Chem. 380, 325–333.
[21] Kratz, P.A., Böttcher, B. and Nassal, M. (1999) Proc. Natl. Acad. Sci. USA 96, 1915–1920.
[22] Cotton, F.A., Hazen Jr., E.E. and Legg, M.J. (1979) Proc. Natl. Acad. Sci. USA 76, 2551–2555.
[23] Tucker, P.W., Hazen Jr., E.E. and Cotton, F.A. (1979) Mol. Cell Biochem. 23, 67–86.
[24] Nassal, M. (1988) Gene 66, 279–294.
[25] Weber, D.J., Serpersu, E.H., Shortle, D. and Mildvan, A.S. (1990) Biochemistry 29, 8632–8642.
[26] Weber, D.J., Meeker, A.K. and Mildvan, A.S. (1991) Biochemistry 30, 6103–6114.
[27] Deuschle, U., Kammerer, W., Gentz, R. and Bujard, H. (1986) EMBO J. 5, 2987–2994.
[28] Laemmli, U.K. (1970) Nature 227, 680–685.
[29] Sällberg, M., Ruden, U., Magnius, L.O., Harthus, H.P., Noah, M. and Wahren, B. (1991) J. Med. Virol. 33, 248–252.
[30] Pushko, P., Sällberg, M., Borisova, G., Ruden, U., Bichko, V., Wahren, B., Pumpens, P. and Magnius, L. (1994) Virology 202, 912–920.
[31] Serwer, P., Khan, S.A. and Griess, G.A. (1995) J. Chromatogr. A 698, 251–261.
[32] Baker, T.S., Olson, N.H. and Fuller, S.D. (1999) Microbiol. Mol. Biol. Rev. 63, 862–922.
[33] Wingfield, P.T., Stahl, S.J., Williams, R.W. and Steven, A.C. (1995) Biochemistry 34, 4919–4932.
[34] Milich, D.R., Chen, M., Schodel, F., Peterson, D.L., Jones, J.E.

and Hughes, J.L. (1997) Proc. Natl. Acad. Sci. USA 94, 14648–14653.
[35] Seifer, M. and Standring, D.N. (1994) J. Virol. 68, 5548–5555.
[36] Boeke, J.D. and Hahn, B. (1996) Trends Microbiol. 4, 421–426.
[37] Natsoulis, G. and Boeke, J.D. (1991) Nature 352, 632–635.
[38] Natsoulis, G., Seshaiah, P., Federspiel, M.J., Rein, A., Hughes, S.H. and Boeke, J.D. (1995) Proc. Natl. Acad. Sci. USA 92, 364–368.
[39] VanBrocklin, M., Ferris, A.L., Hughes, S.H. and Federspiel, M.J. (1997) J. Virol. 71, 3312–3318.